IET Control Theory & Applications

Research Article

Stable adaptive NSOF domain FOPID controller for a class of non-linear systems

ISSN 1751-8644
Received on 25th July 2017
Revised 11th February 2018
Accepted on 1st March 2018
E-First on 3rd April 2018
doi: 10.1049/iet-cta.2017.0732
www.ietdl.org

Debasish Biswas[1] ✉, *Kaushik Das Sharma*[2], *Gautam Sarkar*[2]

[1]*Department of Electrical Engineering, Techno India College of Technology, Newtown, Kolkata, India*

[2]*Department of Applied Physics, University of Calcutta, 92 APC Road, Kolkata, India*

✉ *E-mail: debasishmee@hotmail.com*

Abstract: The present study proposes a new approach for designing stable adaptive fractional-order proportional–integral–derivative (FOPID) controllers, which employs non-sinusoidal orthogonal function (NSOF) domain-based design approach. The objective is to design a self-adaptive FOPID controller such that the designed controller can guarantee desired stability and simultaneously it can provide satisfactory transient performance. The proposed design methodology simplifies and eliminates the complexity of solving fractional-order system dynamics by converting it into the algebraic vector–matrix equation with the help of NSOF. The conventional FOPID, NSOF-based FOPID and NSOF-based adaptive FOPID controllers are implemented for benchmark simulation case studies and real-life experimentation and their results demonstrate the usefulness of the proposed approach.

1 Introduction

We are interested in developing a technique for controller design that achieves boundedness of the output trajectory for a class of non-linear plant. For the specific class of non-linear plant, boundedness of trajectories demands both zero tracking error and minimisation of performance specification (like integral absolute error (IAE) or integral squared error [1–4]. Optimisation of the performance specification for the tracking control system requires a controller, which can give sufficient amount lead–lag compensation to meet the transient and steady-state specification as well as compensation to the non-linearity of the plant via feedback linearisation technique [2]. In real-life control problems, performance and robustness of control systems are affected by non-linearities of the plant, model or parameter uncertainties, load disturbance and high-frequency noise and as a result, the performance of the controller degrades [5, 6].

A wide range of control problems are utilising the advantage of classical proportional–integral–derivative (PID) controller to achieve the required performance specification and robustness in the presence of non-linearities in the plant, model or parameter uncertainties, load disturbance and high-frequency noise [7–12]. Recent studies in the past decade show that the action of fractional-order PID (FOPID) controller with five unknown parameters will have a more precise effect [13] instead of three parameters classical PID controller. Other fractional-order controller such as fractional-order lead–lag compensator [14] different generation of CRONE controllers [15], optimal fractional-order controllers [16] have been studied in the past decade as a generalisation of integer-order controller to enhance the performance of control systems. So, if the feedback linearisation scheme is applied to optimise the performance and robustness of a tracking control system, the generalised version of PID controller can make a major contribution.

The fractional-order controller first analysed in the frequency domain with the help of a Bode or a Nyquist diagram. The design problem of feedback amplifier whose performance is invariant of changes of gain leads to Bode's ideal transfer function [17] which is a fractional integrator. Oustaloup [18] demonstrated that the performance of CRONE controller is superior over the PID controller. Podlubny proposed [19] the tuning technique of FOPID controller for a linear constant coefficient fractional-order plant to minimise the tracking error. This technique shows the local stability to a unit step signal with better performance than a classical PID controller. Monje *et al.* [6] discussed the ability to cancel steady-steady error and output convergence using a fractional-order integral controller or band-limited integral controller. The band-limitation of derivative controller ensures the noise cancellation at high frequency.

The most common technique to realise the FOPID controller is to replace the fractional-order transfer function by an integer-order transfer function whose characteristics are close enough to the desired. In the analytical tuning technique, the FOPID controller provides five non-linear equations to meet the desired gain and the phase margin [6]. If the S-shaped step response of the plant is available then FOPID controller can be tuned using rule-based techniques otherwise optimisation techniques are useful for tuning the controller [6, 20]. In recent studies, the continuous approximation of the FOPID controller is implemented via different types of numerical techniques in discrete domain [21].

So, it is clear that the application of FOPID controller is restricted to linear or time delay system whose analysis is based on direct frequency domain specifications and indirectly on time domain specifications. The design criterion is selected via frequency domain specifications. Also, it is established that FOPID controller [6, 20, 22–25] has the capability to meet exact performance specification by providing a continuous surface in phase angle via fractional-order integral (I) or derivative (D) controller [19, 26] in the case of wide range of control problems.

Podlubny [27, 28] and others reveal the geometric and physical interpretation, the hereditary property of the fractional-order integrator if the variation of the order of the integrator is within $(-1, 0)$ and order of the differentiator within (0,1). This property of fractional-order differintegral is utilised in the FOPID controller for different types of linear system in the frequency domain via approximated transfer function techniques. Then time-domain analysis is done based on the frequency domain data. They also proposed a matrix approach to solving differential equation of integer or non-integer order with initial and boundary values [29]. Here, the operational matrix for integration and differentiation is based on forward or backward difference method. These numerical methods of integration are based on the difference formulae. It is restricted to a linear discrete difference equation. To the best of our knowledge, the behaviour of the FOPID controller with the non-linear system in the time domain is yet to reveal.

The performance of the controller improves relatively for a piecewise linearisable system if the gain scheduling technique is applied in the cost of high computational time and manual interventions for generating the proper control signal to meet the desired specification, in particular, operating zone [30–32]. Synthesis of adaptive controller can overcome this disadvantage [3, 33, 34]. Backstepping method or Lyapunov-based strategies have been utilised to design an adaptive controller to keep zero tracking error and minimum performance specification [4, 35, 36]. The control technique, provided by both of these methodologies, is similar to the PID control action. In the backstepping method, the convergence rate of controller parameters with varying reference signal depends on the value of learning factor. So the performance of the controller and its stability are dependent on the initial guess of controller parameters. While Lyapunov-based synthesis of the self-tuning PID controller demands supervisory control to guarantee closed-loop stability because discontinuity in phase lead or lag due to integer-order integral or derivative controller degrades the performance of the self-tuned PID controller. So, the design technique of adaptive FOPID controller to control a special class of non-linear plant will be a challenging task. Because the complexity in the derivation of the global asymptotic stability condition increases due to the insertion of fractional calculus in system dynamics. Also, the stability analysis of non-linear plant with a fractional-order PID controller in the feed forward path depends on the existence of a Lyapunov candidate function [37, 38].

Many members of non-sinusoidal piecewise constant orthogonal function are binary valued and indicate the applicability in the analysis and synthesis of digital control systems in a piecewise constant manner. The non-sinusoidal orthogonal function (NSOF) sets like Walsh function, Haar function, block pulse functions [39], sample and hold functions (SHFs) [40, 41], triangular functions (TFs) [42] and hybrid functions (HFs) [43, 44] have already been used to analysis and synthesis of linear/non-linear continuous-time control system including time-invariant, time-varying, time-delay or multi-delay system using matrix operation techniques. The operational matrices for integration and differentiation are developed from the NSOF domain representation after the integration of each basis function. In the NSOF domain, state-space representation of the system dynamics is converted into the algebraic vector–matrix equation. The integer-order operational matrix for integration and differentiation is successfully implemented to solve the different variants of linear system dynamics. However, the application area of the techniques is restricted to an integer-order linear control system.

This paper proposes an alternative approach of designing the FOPID controller for a class of non-linear systems subjected to tracking a reference signal. Here, the objective is to achieve boundedness of the output trajectory with minimum tracking error using the philosophy of feedback linearisation technique. This scheme always gives a linear error dynamics with ideal control law in the time domain for a class of non-linear systems. The design of optimal FOPID controller with the help of quasi-continuous NSOF domain considering minimum approximation error is introduced here. Although, the global stability conditions of NSOF domain-based techniques to solve real-life control problems are not available in the literature.

This paper utilises SHF sets in conjunction with TF sets, as members of NSOF sets, to form a hybrid NSOF [44, 45] for designing the FOPID controllers. The application of NSOF domain-based transformation technique on the proposed scheme reveals the contributions which are listed below:

i. The system dynamics is an algebraic vector–matrix equation in the NSOF domain instead of the fractional-order system in the sinusoidal domain.
ii. The internal structure of FOPID controller matrix in the NSOF domain is sufficient to redesign the implementation technique of non-causal convolution in real-life problem considering minimum approximation error, i.e. do not sacrifice the performances of the controller in real-life applications.
iii. The HF domain dynamics of the proposed scheme is a simple algebraic vector–matrix equation in the state space and is used in Lyapunov re-design technique to find the global asymptotic stability condition.
iv. Lyapunov-based stability analysis technique in quasi-continuous NSOF domain gives the adaptation rule of the parameters of FOPID controller and results are represented in the continuous time domain.
v. The adaptation rules are independent of gamma function that means the proposed scheme eliminates the complexity of fractional-order calculations.
vi. The tuned parameters of FOPID controller using new adaption rule fulfils the two competing requirements: (1) guarantee the stability of the designed controller and overall system and (2) achieve a good of transient performance without any initial guess of controller parameters.

The proposed design strategy has been implemented for different benchmark case studies and also experimented on a real-life problem. The proposed HF-based non-adaptive and adaptive FOPID control strategies are compared with the controllers designed by conventional PID and FOPID concepts. The obtained results demonstrate, on the whole, the superiority of the HF-based adaptive FOPID approach over the other approaches. The remaining of the paper organised as follows: The detailed discussion on control objective is given in Section 2. A set of NSOF is named as hybrid function and its characteristics are discussed in Section 3. Adaptation rules and implementation technique of FOPID controller using the NSOF domain are given in Section 4. In Section 5, controller, design examples are studied and finally, conclusions are presented in Section 6.

2 Problem formulation and FOPID controller

Let us consider that the control objective is to design an adaptive strategy for a nth-order non-linear plant given as [4, 46]

$$\begin{cases} x^{(n)} = f(x) + bu \\ y = x \end{cases} \tag{1}$$

where $f(\cdot)$ is an unknown continuous function, $u \in \mathbb{R}^1$ and $y \in \mathbb{R}^1$ are the input and the output of the plant, respectively, and b is an unknown positive constant. It is assumed that the state vector is given as $\mathbf{x} = [x_1, x_2, \ldots, x_n]^{\mathrm{T}} = [x, \dot{x}, \ldots, x^{(n)}]^{\mathrm{T}} \in \mathbb{R}^n$. The dynamical system is controllable, if $b \neq 0$. Thus, without loss of generality we can assume that $b > 0$.

The control objective is to force the plant output $y(t)$ to follow a given bounded reference signal $y_m(t)$ under the constraints that all closed-loop variables involved must be bounded to guarantee the closed-loop stability of the system. Thus, the tracking error is $e(t) = y_m(t) - y(t)$ must be minimised in terms of the performance index.

The objective is to design a stable controller for the system described here. The system must follow the conditions as:

1. The closed-loop system must be globally stable in the sense that all variables must be uniformly bounded and $u \leq M_u < \infty$ where M_u is set by the designer.
2. The tracking error $e(t)$ should be as small as possible under the constraints in (1).

The ideal control law [4] for the system in (1) is given as

$$u^* = \frac{1}{b}\left[-f(\mathbf{x}) + y_m^{(n)} + \mathbf{k}^{\mathrm{T}}\mathbf{e}\right] \tag{2}$$

where $y_m^{(n)}$ is the nth derivative of the output of the reference model/the reference signal.

In case of a controller to accomplish these control objectives, let the error vector be $\mathbf{e} = [e, \dot{e}, \ldots, e^{(n-1)}]^{\mathrm{T}}$ and $\mathbf{k} = [k_1, k_2, \ldots, k_n]^{\mathrm{T}} \in \mathbb{R}^n$ be such that all the roots of the Hurwitz polynomial $s^n + k_n s^{(n-1)} + \cdots + k_2 s + k_1$ are in the left half of s-plane. For some specific class of plants, let the error differential equation is as $e^{(n)} = -k_1 e - k_2 \dot{e} - \cdots - k_n e^{(n-1)}$.

This definition implies that u^* guarantees perfect tracking, i.e. $y(t) \equiv y_m(t)$ if $\lim_{t \to \infty} e(t) = 0$. Here the vector k describes the desired closed-loop dynamics for the plant error. In practical situations, since f and b are not known precisely, the ideal u^* of cannot be implemented in real practice. Thus, a suitable solution is required to design a controller to approximate this optimal control law. Now, utilising (2), the error differential equation will be

$$\begin{aligned} e^{(n)}(t) &= -\mathbf{k}^{\mathrm{T}}\mathbf{e}(t) - b[u^* - u_c(t)] \\ \dot{\mathbf{e}}(t) &= \mathbf{\Lambda_c e}(t) + b_c[u^* - u_c(t)] \end{aligned} \tag{3}$$

where

$$\Lambda_c = \begin{bmatrix} 0 & 1 & 0 & \cdots & 0 \\ 0 & 0 & 1 & \cdots & 0 \\ \vdots & \vdots & \vdots & \ddots & \vdots \\ 0 & 0 & 0 & \ldots & 0 \\ -k_1 & -k_2 & -k_3 & \cdots & -k_n \end{bmatrix}, \quad b_c = \begin{bmatrix} 0 \\ 0 \\ 0 \\ \vdots \\ b \end{bmatrix}$$

2.1 Fractional-order PID controller

The designing of FOPID controller for an integer-order plant is more common issue than other combination of plant and controller [19]. If the input to the FOPID controller is $e(t)$and output is $u_{\mathrm{FOPID}}(t)$ then

$$u_{\mathrm{FOPID}}(t) = K_{\mathrm{P}} e(t) + K_{\mathrm{I}} D^{\alpha} e(t) + K_{\mathrm{D}} D^{\beta} e(t) \tag{4}$$

where $K_{\mathrm{P}}, K_{\mathrm{I}}$ and K_{D} are the gains of proportional, integral and derivative controllers, respectively, and D^{α} and D^{β} are the operator of fractional-order integration and derivative, respectively, with $\alpha < 0$ and $\beta > 0$. If the operators of FOPID controller are realised via Reimann–Liouville (RL) and Caputo method or Grunwald–Letnikov (GL) [47–49] method, analysis must be done using convolution operation or considering time-delay in the system dynamics.

2.2 Non-linear system with fractional-order PID controller

The error dynamics of the system in (3) with a FOPID controller is as follows:

$$\dot{\mathbf{e}}(t) = \mathbf{\Lambda_c e}(t) + b_c[u^* - u_{\mathrm{FOPID}}(t)]$$

Now, using (4), we get

$$\dot{\mathbf{e}}(t) = \mathbf{\Lambda_c e}(t) + b_c[K_{\mathrm{P}} + K_{\mathrm{I}} D^{\alpha} + K_{\mathrm{D}} D^{\beta}](e^*(t) - e(t)) \tag{5}$$

Here, the objective is to tune the parameters of the FOPID controller in such way that tracking error will be minimum and the response of the system will be bounded while the controller will (i) take care of robustness of the system if plant gain is changing in nature, (ii) cancel the steady-state error, (iii) concern about output disturbance, (iv) minimise the of high-frequency noise and (v) minimise the effect of non-linearity via feedback linearisation. Monje *et al* [6] already discussed how to handle the first four constrains via frequency domain analysis. However, the difficulty arises during the analysis of the conditions through continuous time domain when the plant is non-linear. Due to the presence of the fractional-order operators of FOPID controller, the analytic solution and condition of stability of the fractional-order dynamics of the above expression include the gamma function. To get rid of this major disadvantage of the fractional-order system, an efficient and simple alternative transformation technique is applied on system dynamics to fulfil the objective of this paper. After a brief discussion about the NSOF domain and its operators in the next section, the system dynamics will be transformed in the NSOF domain for further analysis.

3 NSOF domain and its operators – a preliminary idea

3.1 Function approximation via HF domain [44]

A square integrable time function $f(t)$ of Lebesgue measure may be expanded into SHF (member of piecewise constant basis function (PCBF) family) series or TF (member of piecewise linear basis function (PLBF) family) series in the time interval $[0, T)$ using m number of component functions.

The combination of SHF (PCBF) and RHTF (PLBF) set can be considered as hybrid function (HF) set which is another member of PLBF family. Here, the RHTF set is simply known as TF set. The HF series of a square integrable function $f(t)$ is

$$f(t) \simeq f_{\mathrm{HF}} = \mathbf{F}_S^T \mathbf{S}_{(m)}(t) + \mathbf{F}_T^T \mathbf{T}_{(m)}(t) \tag{6}$$

where $\mathbf{F}_S^T = [f_{S0} \;\; f_{S1} \;\; \cdots \;\; f_{Si} \;\; \cdots \;\; f_{S(m-1)}]$, $\mathbf{F}_T^T = [f_{T0} \;\; f_{T1} \;\; \cdots \;\; f_{Ti} \;\; \cdots \;\; f_{T(m-1)}]$ and $f_{Si} \triangleq f(ih)$ and $f_{Ti} \triangleq f((i+1)h) - f(ih)$ and the relation $f_{Ti} \triangleq f_{S(i+1)} - f_{Si}$ holds between f_{Si} and f_{Ti}, the minimum approximation error is

$$w(t) = f(t) - f_{\mathrm{HF}}$$

The HF domain operational matrix for integration and differentiation can be used to analyse the dynamic system by transforming it into the algebraic vector–matrix equation. For higher-order system, one-shot operation matrix for integration and differentiation is also advantageous [44]. However, the disadvantage is that it is restricted to integer-order system dynamics. So, it is necessary to find the generalised operational matrix for integration and differentiation which has the property to cope up with higher-order system either integer- or fractional-order system.

3.2 Integration and differentiation in HF domain [44, 45]

Both the RL fractional integral and Caputo fractional derivative are based on convolution integral [21, 47]. These convolution processes are causal in nature and increase complexity in further analysis. The advantage of HF domain method is that from the basic principle of derivative or integration we can find the fractional-order operational matrix for derivative or integration in the HF domain. This operational matrix is known as a fractional-order differintegral matrix in the quasi-continuous time domain. Using the forward difference method and first principle of derivative, the nth-order derivative of $f(t)$ is

$$D_t^n f(t) \triangleq \lim_{\delta t \to 0} (\delta t)^{-n} \sum_{j=0}^{n} (-1)^j \binom{q}{j} f(t + (n-j)\delta t) \tag{7}$$

where n is any positive integer. Binomial coefficients are used to represent weights of the function $f(t)$ at different stages. In order to apply the boundary conditions in differentiation formula in (7), we can refer the curve of $f(t)$. If the function $f(t)$ has an upper limit T and lower limit a, we have, $\delta t = h$. For $(m+1)$ number of samples, the general formula of nth-order derivative of $f(t)$ is

$$\begin{aligned} {}_aD_T^n f(t) \triangleq &\lim_{((T-a)/m) \to 0} \left(\frac{T-a}{m}\right)^{-n} \sum_{j=0}^{m} (-1)^j \\ &\times \frac{\Gamma(n+1)}{\Gamma(n-j+1)\Gamma(j+1)} f\left(t + (n-j)\left[\frac{T-a}{m}\right]\right) \end{aligned} \tag{8}$$

where $\Gamma(\cdot)$ represents the gamma function. Equations (7) and (8) are equivalent because

$$(-1)^j \frac{\Gamma(n+1)}{\Gamma(n-j+1)\Gamma(j+1)} = 0 \quad \text{if } j > n\,.$$

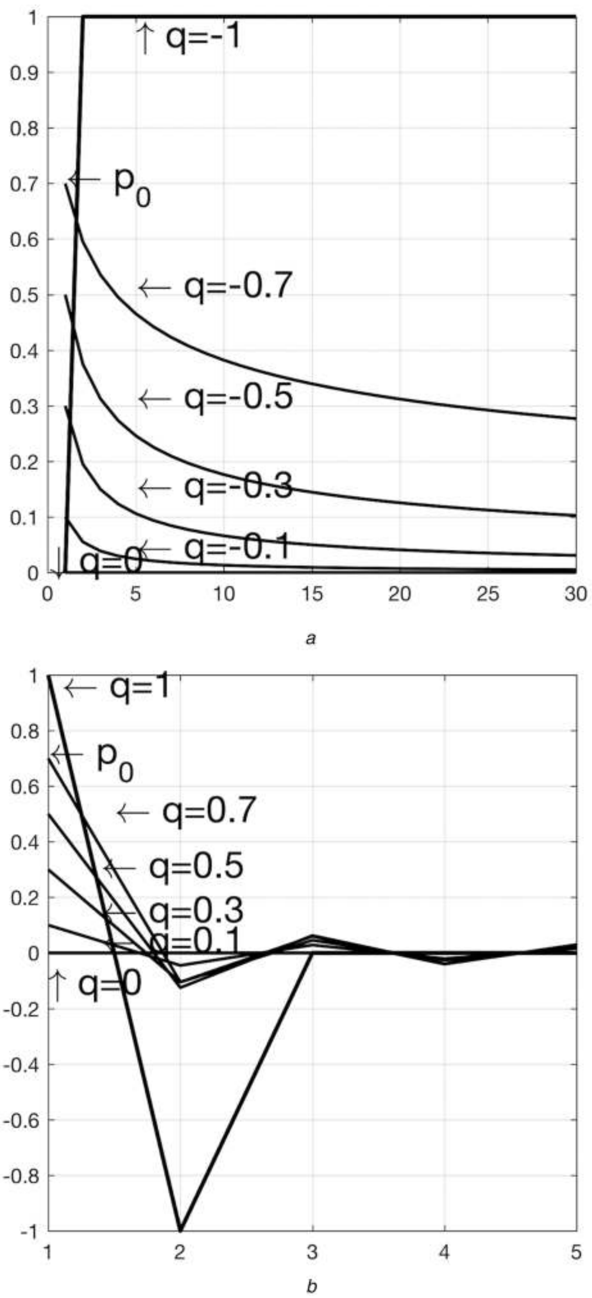

Fig. 1 *Variation of p using* □
(a) 30 samples for different negative values of q within $(-1, 0)$, ***(b)*** 5 samples for different positive values of q within $(0, 1)$

The formula of (8) is applicable for any positive integer n to evaluate the derivative of integer order. We can also use (8) to find integration of the function $f(t)$ if n is negative integer. For negative value of n, (8) becomes

$$\begin{aligned} {}_aD_T^n f(t) \triangleq & \lim_{((T-a)/m)\to 0} \left(\frac{T-a}{m}\right)^{-n} \sum_{j=0}^{m} (-1)^j \frac{\Gamma(n+1)}{\Gamma(n)\Gamma(j+1)} \\ & \times f\left(t+(n-j)\left[\frac{T-a}{m}\right]\right) \end{aligned} \tag{9}$$

When n is the negative integer, (9) can be used to find an integration of $f(t)$. So, using (8) or (9), both differentiation and integration of the function $f(t)$ can be found numerically and is now the formula of differintegral of the function $f(t)$ considering q is an arbitrary number. Now the simplified form of qth-order diferintegral of the function $f(t)$ is

$${}_aD_T^q f(t) \simeq \lim_{h\to 0} h^{-q} \sum_{j=0}^{m} (-1)^j p_j f(t+(q-j)h]) \tag{10}$$

where

$$p_i = \begin{cases} \dfrac{\Gamma(q+i)}{\Gamma(q)\Gamma(i+1)}, & q \text{ is negative} \\ \dfrac{\Gamma(q+1)}{\Gamma(q-i+1)\Gamma(i+1)}, & q \text{ is positive} \end{cases}$$

For $(m+1)$ number of samples, total number of component functions in the HF domain is m. Differ–integral of the function $f(t)$ in the time interval $[a, T)$ is given as follows [29, 44, 45]:

$$\begin{aligned} {}_a\mathbf{D}_T^q f(t) = & \frac{d^q f(t)}{dt^q}\Big|_{t\in[a,T)} \simeq \begin{bmatrix} f_{S0} & f_{S1} & \cdots & f_{S(m-1)} \end{bmatrix} h^{-q} \\ & \times \begin{bmatrix} p_0 & p_1 & p_2 & \cdots & p_{m-2} & p_{m-1} \\ 0 & p_0 & p_1 & \cdots & p_{m-3} & p_{m-2} \\ 0 & 0 & p_0 & \cdots & p_{m-3} & p_{m-4} \\ \vdots & \vdots & \vdots & \ddots & \vdots & \vdots \\ 0 & 0 & 0 & \cdots & p_0 & p_1 \\ 0 & 0 & 0 & \cdots & 0 & p_0 \end{bmatrix} \\ & + \begin{bmatrix} f_{T0} & f_{T1} & \cdots & f_{T(m-1)} \end{bmatrix} h^{-q} \\ & \times \begin{bmatrix} p_{10} & p_{21} & p_{32} & \cdots & p_{(m-1)(m-2)} & p_{(m)(m-1)} \\ 0 & p_{10} & p_{21} & \cdots & p_{(m-2)(m-3)} & p_{(m-1)(m-2)} \\ 0 & 0 & p_{10} & \cdots & p_{(m-2)(m-3)} & p_{(m-3)(m-4)} \\ \vdots & \vdots & \vdots & \ddots & \vdots & \vdots \\ 0 & 0 & 0 & \cdots & p_{10} & p_{21} \\ 0 & 0 & 0 & \cdots & 0 & p_{10} \end{bmatrix} \end{aligned} \tag{11}$$

Here $-\infty \le q \le \infty$ and using (11), we can find the fractional-order differ–integral of $f(t)$ in the continuous time domain and $p_{ij} = p_j - p_i, i = 0, 1, 2, \ldots, (m-1)$ and $j = 1, 2, \ldots, m$ Using (6) and (11) we get,

$$a\mathbf{D}_T^q f(t) \simeq \mathbf{F}_S^T \mathbf{D}_{\text{FS}}^q \mathbf{S}_{(m)}(t) + \mathbf{F}_T^T \mathbf{D}_{\text{FT}}^q \mathbf{T}_{(m)}(t) \tag{12}$$

where $\mathbf{D}_{\text{FS}}^q$ and $\mathbf{D}_{\text{FT}}^q$ are the operational matrices of differ–integral of an order q in the SHF and TF domains, respectively.

The result in (11) can be used to find the operational matrix of the FOPID controller using the time-domain description of the FOPID controller in (4).

When the order of q in (12) is equal to minus one, all the elements above the main diagonal of the SHF domain integration matrix $\mathbf{D}_{\text{FS}}^q$ is equal to one and the TF domain integration matrix $\mathbf{D}_{\text{FT}}^q$ becomes an identity matrix [44]. When the HF domain integration matrices are operating on input function, it accumulates the whole history of the input function.

As q tends to zero, all other elements except the elements of the diagonal elements of the SHF domain integration matrix $\mathbf{D}_{\text{FS}}^q$ and the TF domain integration matrix $\mathbf{D}_{FT}^q$ are equal to zero. When these matrices are operated on any input function, the output is one-sided delta function which corresponds to a process with absolutely no memory.

Finally, for $-1 < q < 0$, the nature of weightage of samples of input function can be determined from the Fig. 1*a* for each value of q. When the SHF domain integration matrix $\mathbf{D}_{\text{FS}}^q$ and the TF domain integration matrix $\mathbf{D}_{\text{FT}}^q$ are operating on any input function, it partially captures the past history of the function. At any instant of time, the present value of the input function is given a maximum weight and the past states are given less weightage depending on the order of the fractional integration as shown in (11). The weightage of input function can be determined from Fig. 1*b* when

$0 < q < 1$. Now, $\mathbf{D}_{\mathrm{FS}}^{q}$ and $\mathbf{D}_{\mathrm{FT}}^{q}$ will operate as differentiation matrix. The weightage of the input function is calculated using the properties of the HF domain functions [44] considering 150 component functions.

4 Main result

The plant dynamics as described in (5) can be expressed in the HF domain for further development of controllers [44, 45]. In the HF domain, the weighting coefficients of state vector $\mathbf{e}(t)$, control vector $u(t)$, ideal control signal $u^{*}(t)$, output signal $y(t)$, approximation error $w(t)$ are n-vectors and form the $(i+1)$th column of the $\mathbf{E}_S$, $\mathbf{U}_S$, $\mathbf{U}_S^{*}$, $\mathbf{Y}_S$, $\mathbf{W}_S$, $\mathbf{E}_T$, $\mathbf{U}_T$, $\mathbf{U}_T^{*}$, $\mathbf{Y}_T$, $\mathbf{W}_T$ matrices, respectively. Now, including the minimum approximation error $w(t)$, the closed-loop dynamics in the HF domain is given by

$$
\begin{aligned}
&\mathbf{E}_S\mathbf{D}_{\mathrm{FS}}^{1}\mathbf{S}(t)+\mathbf{E}_T\mathbf{D}_{\mathrm{FT}}^{1}\mathbf{T}(t)=\Lambda_c(\mathbf{E}_S\mathbf{S}(t)+\mathbf{E}_T\mathbf{T}(t))\\
&\quad+b_c[(\mathbf{U}_S^{*\,T}-\mathbf{U}_S^{T})\mathbf{S}(t)-(\mathbf{U}_T^{*}-\mathbf{U}_T^{T})\mathbf{T}(t)]\\
&\quad+\mathbf{W}_S^{T}\mathbf{S}(t)+\mathbf{W}_T^{T}\mathbf{T}(t)
\end{aligned}
$$

Lemma 1: Consider the time-domain expression of the FOPID controller in (4). The input to the FOPID controller is $e(t)$ and output is $u(t)$. If the differ–integral operator in (11) of the HF domain is applied on the FOPID controller (4), the expression of the HF domain FOPID controller is a simple algebraic equation.

Proof: Using the operational matrices of the HF domain, the representation of the FOPID controller in (4) in the HF domain is as follows:

$$
\begin{aligned}
u_{\mathrm{FOPID}}(t)\simeq\ &\mathbf{U}_S^{T}(S)(t)+\mathbf{U}_T^{T}(T)(t)\\
=&\left(K_{\mathrm{P}}\mathbf{E}_{1S}^{\mathrm{T}}I_{nxm}+K_{\mathrm{I}}\mathbf{E}_{1S}^{\mathrm{T}}\mathbf{D}_{\mathrm{FS}}^{\alpha}+K_{\mathrm{D}}\mathbf{E}_{1S}^{\mathrm{T}}\mathbf{D}_{\mathrm{FS}}^{\beta}\right)\mathbf{S}(t)\\
&+\left(K_{\mathrm{P}}\mathbf{E}_{1T}^{\mathrm{T}}I_{nxm}+K_{\mathrm{I}}\mathbf{E}_{1T}\mathbf{D}_{\mathrm{FT}}^{\alpha}+K_{\mathrm{D}}\mathbf{E}_{1T}^{\mathrm{T}}\mathbf{D}_{\mathrm{FT}}^{\beta}\right)\mathbf{T}(t)
\end{aligned}
\quad (13)
$$

where $\mathbf{D}_{\mathrm{FS}}^{\alpha}$ and $\mathbf{D}_{\mathrm{FS}}^{\beta}$ are the SHF domain operational matrices for fractional-order integration and derivative, respectively. $\mathbf{D}_{\mathrm{FT}}^{\alpha}$ and $\mathbf{D}_{\mathrm{FT}}^{\beta}$ are the TF domain operational matrices for fractional-order integration and derivative, respectively.
Now, taking $m=2, \alpha<0, \beta>0$, we get

$$
\begin{aligned}
&\mathbf{U}_{S_{(2)}}^{\mathrm{T}}\mathbf{S}_{(2)}(t)+\mathbf{U}_{T_{(2)}}^{\mathrm{T}}\mathbf{T}_{(2)}(t)=\begin{bmatrix}e_{S0} & e_{S1}\end{bmatrix}\\
&\times\begin{bmatrix}K_{\mathrm{P}}+p_{\alpha0}K_{\mathrm{I}}h_F^{\alpha}+p_{\beta0}K_{\mathrm{D}}h_F^{\beta} & p_{\alpha1}K_{\mathrm{I}}h_F^{\alpha}+p_{\beta1}K_{\mathrm{D}}h_F^{\beta}\\ 0 & K_{\mathrm{P}}+p_{\alpha0}K_{\mathrm{I}}h_F^{\alpha}+p_{\beta0}K_{\mathrm{D}}h_F^{\beta}\end{bmatrix}\\
&+\begin{bmatrix}e_{T0} & e_{T1}\end{bmatrix}\\
&\times\begin{bmatrix}K_{\mathrm{P}}+p_{\alpha10}K_{\mathrm{I}}h_F^{\alpha}+p_{\beta10}K_{\mathrm{D}}h_F^{\beta} & p_{\alpha12}K_{\mathrm{I}}h_F^{\alpha}+p_{\beta12}K_{\mathrm{D}}h_F^{\beta}\\ 0 & K_{\mathrm{P}}+p_{\alpha10}K_{\mathrm{I}}h_F^{\alpha}+p_{\beta10}K_{\mathrm{D}}h_F^{\beta}\end{bmatrix}
\end{aligned}
\quad (14)
$$

So, using (12), the control signal in the HF domain, in terms of error signal, is

$$
\mathbf{U}_S^{\mathrm{T}}\mathbf{S}(t)+\mathbf{U}_T^{\mathrm{T}}\mathbf{T}(t)=\mathbf{E}_S^{\mathrm{T}}\mathbf{M}_S\mathbf{S}(t)+\mathbf{E}_T^{\mathrm{T}}\mathbf{M}_T\mathbf{T}(t) \quad (15)
$$

where $\mathbf{M}_S$ and $\mathbf{M}_T$ are operational matrices of the FOPID controller in SHF and TF domains, respectively.
The common properties of the FOPID controller like robustness to variation in the gain of the plant, i.e. iso-damping property of time response, high-frequency noise rejection, steady-state error correction, minimisation of non-linearity effect through quasi-continuous time domain are discussed in Section 5 through simulation and real-life control problems using different variants of the HF domain FOPID controller. The expression of the FOPID controller in (14) with the help of Figs. 1*a* and *b* shows that at any instant of time if the range of q is between $(-1, 1)$ then the present sample of error signal is getting the highest weight and the weight of past samples is decreasing exponentially as time increases. If the value of q is equal to -1 then all the samples of the error signal is accumulated by the integrator by providing maximum memory. Whereas if q is decreasing towards 0 the memory power of the integrator is decreasing in nature. So, we can easily correct the steady-state error, effect of output disturbance of the system by controlling the value of q within $(-1, 0)$. On the other hand, Fig. 1*b* shows that the upper limit of the positive value of q (which is 1) will increase the rise time, overshoot of the system but oscillation will be more. If the value of the q is going towards 0, the memory power of the differentiator is increasing. □

Now, putting the expression of HF domain FOPID controller from Lemma 1, the error dynamics in the HF domain becomes

$$
\begin{aligned}
&\mathbf{E}_S\mathbf{D}_{\mathrm{FS}}^{1}\mathbf{S}(t)+\mathbf{E}_T\mathbf{D}_{\mathrm{FT}}^{1}\mathbf{T}(t)\\
&\quad=\left[\Lambda_c\mathbf{E}_S+b_c\mathbf{E}_{1S}^{T}(\mathbf{M}_S^{*}-\mathbf{M}_S)+\mathbf{W}_S^{T}\right]\mathbf{S}(t)\\
&\quad+[\Lambda_c\mathbf{E}_T+b_c\mathbf{E}_{1T}^{T}(\mathbf{M}_T^{*}-\mathbf{M}_T)+\mathbf{W}_T^{T}]\mathbf{T}(t)
\end{aligned}
$$

Now, equating the coefficients of the SHF and TF domains, we get

$$
\begin{cases}
\mathbf{E}_S\mathbf{D}_{\mathrm{FS}}^{1}=\Lambda_c\mathbf{E}_S+b_c\mathbf{E}_{1S}^{T}(\mathbf{M}_S^{*}-\mathbf{M}_S)+\mathbf{W}_S^{T}\\
\mathbf{E}_T\mathbf{D}_{\mathrm{FT}}^{1}=\Lambda_c\mathbf{E}_T+b_c\mathbf{E}_{1T}^{T}(\mathbf{M}_T^{*}-\mathbf{M}_T)+\mathbf{W}_T^{T}
\end{cases}
\quad (16)
$$

where $\mathbf{D}_{\mathrm{FS}}^{1}$ and $\mathbf{D}_{\mathrm{FT}}^{1}$ are the operational matrices of differentiation in the SHF and TF domains, respectively.

4.1 Adaptation rules of FOPID controller

In this section, the stability condition is derived by using the HF domain representation of system dynamics from the understanding of stability in the sense of Lyapunov. Let us define the Lyapunov function of a non-autonomous system as

$$
\begin{aligned}
V_e(t)\simeq\ &\mathbf{V}_{eS}^{T}\mathbf{S}(t)+\mathbf{V}_{eT}^{T}\mathbf{T}(t)\\
&+\frac{1}{2}[\mathbf{E}_S\mathbf{S}(t)+\mathbf{E}_T\mathbf{T}(t)]^{\mathrm{T}}\mathbf{P}[\mathbf{E}_S\mathbf{S}(t)+\mathbf{E}_T\mathbf{T}(t)]\\
&+\frac{b}{2\gamma}[(\mathbf{M}_S^{*}-\mathbf{M}_S)\mathbf{S}(t)+(\mathbf{M}_T^{*}-\mathbf{M}_T)\mathbf{T}(t)]^{\mathrm{T}}\\
&\times[(\mathbf{M}_S^{*}-\mathbf{M}_S)\mathbf{S}(t))+(\mathbf{M}_T^{*}-\mathbf{M}_T)\mathbf{T}(t)]
\end{aligned}
\quad (17)
$$

where $V_e(t)$ is the Lyapunov candidate function, $\mathbf{V}_{eS}^{T}$ and $\mathbf{V}_{eT}^{T}$ are the weighting coefficients of the Lyapunov function in the HF domain, $\mathbf{P}$ is a symmetric positive definite matrix satisfying the Lyapunov equation. Here, $\mathbf{Q}$ is a positive definite matrix. Now, the stability condition can be derived from (16) and (17) with the help of the following lemmas.

Lemma 2: Consider the HF domain representation of the square integrable function $f(t)$ in (6). The quadratic form of function $f(t)$ can also be expressed in the HF domain.

Proof: The quadratic function g_{HF} in terms of f_{HF} is as follows:

$$
\begin{aligned}
g_{\mathrm{HF}}=\frac{1}{2}\mathbf{f}_{\mathrm{HF}}^{\mathrm{T}}\mathbf{P}\mathbf{f}_{\mathrm{HF}}=&\left[\mathbf{F}_S^{T}\mathbf{S}_{(m)}(t)+\mathbf{F}_T^{T}\mathbf{T}_{(m)}(t)\right]^{\mathrm{T}}\mathbf{P}\\
&\times\left[\mathbf{F}_S^{T}\mathbf{S}_{(m)}(t)+\mathbf{F}_T^{T}\mathbf{T}_{(m)}(t)\right]
\end{aligned}
$$

Now, using the properties of HF [45], it can be written as

$$
\begin{aligned}
&=\frac{1}{2}\mathbf{S}^{\mathrm{T}}(t)\left[\mathbf{F}_S^{T}\mathbf{P}\mathbf{F}_S\right]\mathbf{S}(t)+\frac{1}{2}\mathbf{S}^{\mathrm{T}}(t)\left[\mathbf{F}_S^{T}\mathbf{P}\mathbf{F}_T\right]\mathbf{T}(t)\\
&\quad+\frac{1}{2}\mathbf{T}^{\mathrm{T}}(t)\left[\mathbf{F}_T^{T}\mathbf{P}\mathbf{F}_S\right]\mathbf{T}(t)+\frac{1}{2}\mathbf{T}^{\mathrm{T}}(t)\left[\mathbf{F}_T^{T}\mathbf{P}\mathbf{F}_T\right]\mathbf{T}(t)\\
g_{\mathrm{HF}}&=\frac{1}{2}\mathrm{diag}\left[\mathbf{F}_S^{T}\mathbf{P}\mathbf{F}_S\right]\mathbf{S}(t)\\
&\quad+\frac{1}{2}\left[\mathrm{diag}\left[\mathbf{F}_S^{T}\mathbf{P}\mathbf{F}_T\right]+\mathrm{diag}\left[\mathbf{F}_T^{T}\mathbf{P}\mathbf{F}_S\right]+\mathrm{diag}\left[\mathbf{F}_T^{T}\mathbf{P}\mathbf{F}_T\right]\right]\mathbf{T}(t)
\end{aligned}
\quad (18)
$$

□

Lemma 3: Consider the HF domain expression of the square integrable function $f(t)$ in (6). The derivative of quadratic form of $f(t)$ as shown in Lemma 2 can also be expressed in the HF domain

Proof: The derivative of the quadratic form in the HF domain is as follows:

$$\begin{aligned}\frac{\mathrm{d}^q g(t)}{\mathrm{d}t^q} &\simeq \mathbf{G}_S\mathbf{D}_{\mathrm{FS}}^{\mathrm{l}}\mathbf{S}(t) + \mathbf{G}_T\mathbf{D}_{\mathrm{FT}}^{\mathrm{l}}\mathbf{T}(t)\\ &= \frac{1}{2}\left[\mathbf{F}_S^T\mathbf{D}_{\mathrm{FS}}^{\mathrm{l}}\mathbf{S}_{(m)}(t) + \mathbf{F}_T^T\mathbf{D}_{\mathrm{FT}}^{\mathrm{l}}\mathbf{T}_{(m)}(t)\right]^{\mathrm{T}}\mathbf{P}\\ &\quad\times\left[\mathbf{F}_S^T\mathbf{S}_{(m)}(t) + \mathbf{F}_T^T\mathbf{T}_{(m)}(t)\right]\\ &\quad+\left[\mathbf{F}_S^T\mathbf{S}_{(m)}(t) + \mathbf{F}_T^T\mathbf{T}_{(m)}(t)\right]^{\mathrm{T}}\mathbf{P}\\ &\quad\times\left[\mathbf{F}_S^T\mathbf{D}_{FS}^{\mathrm{l}}\mathbf{S}_{(m)}(t) + \mathbf{F}_T^T\mathbf{D}_{FT}^{\mathrm{l}}\mathbf{T}_{(m)}(t)\right]\end{aligned}$$

Using Lemma 2, we get

$$\begin{aligned}&= \mathrm{diag}\left[\left[\mathbf{F}_S^T\mathbf{D}_{FS}^{\mathrm{l}}\right]^{\mathrm{T}}\mathbf{P}\mathbf{F}_S^T\right]\mathbf{S}(t) + \mathrm{diag}\left[\left[\mathbf{F}_S^T\mathbf{D}_{FS}^{\mathrm{l}}\right]^{\mathrm{T}}\mathbf{P}\mathbf{F}_T^T\right]\mathbf{T}(t)\\ &\quad+\mathrm{diag}\left[\left[\mathbf{F}_T^T\mathbf{D}_{FT}^{\mathrm{l}}\right]^{\mathrm{T}}\mathbf{P}\mathbf{F}_S^T\right]\mathbf{T}(t) + \mathrm{diag}\left[\left[\mathbf{F}_T^T\mathbf{D}_{FT}^{\mathrm{l}}\right]^{\mathrm{T}}\mathbf{P}\mathbf{F}_T^T\right]\mathbf{T}(t)\end{aligned} \tag{19}$$

□

The rate vector of the Lyapunov function in (17) is as follows:

$$\begin{aligned}&\mathbf{V}_{eS}^T\mathbf{D}_{\mathrm{FS}}^{\mathrm{l}}\mathbf{S}(t) + \mathbf{V}_{eT}^T\mathbf{D}_{\mathrm{FT}}^{\mathrm{l}}\mathbf{T}(t)\\ &\quad= \frac{1}{2}\left(\mathbf{E}_S\mathbf{D}_{\mathrm{FS}}^{\mathrm{l}}\mathbf{S}(t) + \mathbf{E}_T\mathbf{D}_{\mathrm{FT}}^{\mathrm{l}}\mathbf{T}(t)\right)^T\mathbf{P}\left(\mathbf{E}_S^T\mathbf{S}(t) + \mathbf{E}_T^T\mathbf{T}(t)\right)\\ &\quad+\left(\mathbf{E}_S^T\mathbf{S}(t) + \mathbf{E}_T^T\mathbf{T}(t)\right)^T\mathbf{P}\left(\mathbf{E}_S\mathbf{D}_{\mathrm{FS}}^{\mathrm{l}}\mathbf{S}(t) + \mathbf{E}_T\mathbf{D}_{\mathrm{FT}}^{\mathrm{l}}\mathbf{T}_{(m)}(t)\right)\\ &\quad+\frac{b}{2\gamma}[(\mathbf{M}_S^* - \mathbf{M}_S)\mathbf{D}_{\mathrm{FS}}^{\mathrm{l}}\mathbf{S}(t) + (\mathbf{M}_T^* - \mathbf{M}_T)\mathbf{D}_{\mathrm{FT}}^{\mathrm{l}}\mathbf{T}(t)]^{\mathrm{T}}\\ &\quad\times[(\mathbf{M}_S^* - \mathbf{M}_S)\mathbf{S}(t) + (\mathbf{M}_T^* - \mathbf{M}_T)\mathbf{T}(t)]\\ &\quad+\frac{b}{2\gamma}[(\mathbf{M}_S^* - \mathbf{M}_S)\mathbf{S}(t) + (\mathbf{M}_T^* - \mathbf{M}_T)\mathbf{T}(t)]^{\mathrm{T}}\\ &\quad\times[(\mathbf{M}_S^* - \mathbf{M}_S)\mathbf{D}_{\mathrm{FS}}^{\mathrm{l}}\mathbf{S}(t) + (\mathbf{M}_T^* - \mathbf{M}_T)\mathbf{D}_{\mathrm{FT}}^{\mathrm{l}}\mathbf{T}(t)]\end{aligned} \tag{20}$$

In (20), putting the value from (15) we get

$$\begin{aligned}&= \frac{1}{2}((\Lambda_c\mathbf{E}_S + b_c\mathbf{E}_{1S}^T(\mathbf{M}_S^* - \mathbf{M}_S) + \mathbf{W}_S^T)\mathbf{S}(t)\\ &\quad+(\Lambda_c\mathbf{E}_T + b_c\mathbf{E}_{1T}^T(\mathbf{M}_T^* - \mathbf{M}_T) + \mathbf{W}_T^T)\mathbf{T}(t))^T\\ &\quad\times\mathbf{P}(\mathbf{E}_S^T\mathbf{S}(t) + \mathbf{E}_T^T\mathbf{T}(t)) + \frac{1}{2}(\mathbf{E}_S^T\mathbf{S}(t) + \mathbf{E}_T^T\mathbf{T}(t))^T\mathbf{P}\\ &\quad\times(\Lambda_c\mathbf{E}_S + b_c\mathbf{E}_{1S}^T(\mathbf{M}_S^* - \mathbf{M}_S) + \mathbf{W}_S^T)\mathbf{S}(t)\\ &\quad+(\Lambda_c\mathbf{E}_T + b_c\mathbf{E}_{1T}^T(\mathbf{M}_T^* - \mathbf{M}_T) + \mathbf{W}_T^T)\mathbf{T}(t))^T\\ &\quad+\frac{b}{2\gamma}[-\mathbf{M}_S\mathbf{D}_{\mathrm{FS}}^{\mathrm{l}}\mathbf{S}(t) - \mathbf{M}_T\mathbf{D}_{\mathrm{FT}}^{\mathrm{l}}\mathbf{T}(t)]^{\mathrm{T}}\\ &\quad\times[(\mathbf{M}_S^* - \mathbf{M}_S)\mathbf{S}(t) + \mathbf{M}_T^* - \mathbf{M}_T)\mathbf{T}(t)]\\ &\quad+\frac{b}{2\gamma}[(\mathbf{M}_S^* - \mathbf{M}_S)\mathbf{S}(t) + \mathbf{M}_T^* - \mathbf{M}_T)\mathbf{T}(t)]^{\mathrm{T}}\\ &\quad\times[-\mathbf{M}_S\mathbf{D}_{\mathrm{FS}}^{\mathrm{l}}\mathbf{S}(t) - \mathbf{M}_T\mathbf{D}_{\mathrm{FT}}^{\mathrm{l}}\mathbf{T}(t)]\end{aligned} \tag{21}$$

Applying Lemmas 2 and 3, we get

$$\begin{aligned}&= -\frac{1}{2}(\mathrm{diag}(\mathbf{E}_S^T\mathbf{Q}\mathbf{E}_S)\mathbf{S}(t) + \mathrm{diag}(\mathbf{E}_S^T\mathbf{Q}\mathbf{E}_T)\mathbf{T}(t)\\ &\quad+\mathrm{diag}(\mathbf{E}_T^T\mathbf{Q}\mathbf{E}_S)\mathbf{T}(t) + \mathrm{diag}(\mathbf{E}_T^T\mathbf{Q}\mathbf{E}_T))\mathbf{T}(t)\\ &\quad+\frac{1}{2}(\mathrm{diag}(\mathbf{E}_S^T\mathbf{Q}\mathbf{W}_S)\mathbf{S}(t) + \mathrm{diag}(\mathbf{E}_S^T\mathbf{Q}\mathbf{W}_T)\mathbf{T}(t)\\ &\quad+\mathrm{diag}(\mathbf{E}_T^T\mathbf{Q}\mathbf{W}_S)\mathbf{T}(t) + \mathrm{diag}(\mathbf{E}_T^T\mathbf{Q}\mathbf{W}_T))\mathbf{T}(t)\\ &\quad+\mathrm{diag}\left(-\frac{b}{\gamma}\mathbf{M}_S\mathbf{D}_{\mathrm{FS}}^{\mathrm{l}} + \mathbf{E}_S^T\mathbf{P}b_c\mathbf{E}_{1S}\right)(\mathbf{M}_S^* - \mathbf{M}_S)\mathbf{S}(t)\\ &\quad+\mathrm{diag}(-\frac{b}{\gamma}\mathbf{M}_T\mathbf{D}_{\mathrm{FT}}^{\mathrm{l}} + \mathbf{E}_S^T\mathbf{P}b_c\mathbf{E}_{1T})(\mathbf{M}_S^* - \mathbf{M}_S)\mathbf{T}(t)\\ &\quad+\mathrm{diag}\left(-\frac{b}{\gamma}\mathbf{M}_S\mathbf{D}_{\mathrm{FS}}^{\mathrm{l}} + \mathbf{E}_T^T\mathbf{P}b_c\mathbf{E}_{1S}\right)(\mathbf{M}_T^* - \mathbf{M}_T)\mathbf{T}(t)\\ &\quad+\mathrm{diag}\left(-\frac{b}{\gamma}\mathbf{M}_T\mathbf{D}_{\mathrm{FT}}^{\mathrm{l}} + \mathbf{E}_T^T\mathbf{P}b_c\mathbf{E}_{1T}\right)(\mathbf{M}_T^* - \mathbf{M}_T)\mathbf{T}(t)\end{aligned} \tag{22}$$

An equivalent continuous domain representation of the above quasi-continuous (22) is as follows:

$$\begin{aligned}\dot{V}_e(t) &= -\frac{1}{2}\mathbf{e}^{\mathrm{T}}\mathbf{Q}\mathbf{e} + \mathbf{e}^{\mathrm{T}}\mathbf{P}\mathbf{w}\\ &\quad+\left(-\frac{b}{\gamma}\frac{\mathrm{d}m_F(t)}{\mathrm{d}t} + \mathbf{e}^{\mathrm{T}}\mathbf{P}b_ce)(m_F^*(t) - m_F(t)\right)\end{aligned} \tag{23}$$

Now, if $\dot{V}_e(t) < 0$ then V_e is minimum. It implies the minimisation of the tracking error $e(t)$. As a consequence, the difference between $m_F^*(t)$ and $m_F(t)$ will be minimum, where $m_F(t)$ is the function consisting of parameters of the FOPID controller and is adaptive in nature. For the negative value of $\dot{V}_e(t)$, we have to choose an appropriate adaptation rule for the parameters of the FOPID controller from the above expression and the number of HF domain components must be high enough to minimise the approximation error. The first term $-\frac{1}{2}\mathbf{e}^{\mathrm{T}}\mathbf{Q}\mathbf{e}$ itself is negative, the second term $|\mathbf{e}^{\mathrm{T}}\mathbf{P}\mathbf{w}|$ will be minimum if the number HF domain components is chosen suitably or sufficiently large, and will be less than $|\frac{1}{2}\mathbf{e}^{\mathrm{T}}\mathbf{Q}\mathbf{e}|$, finally if the third item is equal to zero then $\dot{V}_e(t)$ will be less than zero and (23) becomes

$$\dot{V}_e(t) = -\frac{1}{2}\mathbf{e}^{\mathrm{T}}\mathbf{Q}\mathbf{e} + \frac{1}{2}\mathbf{e}^{\mathrm{T}}\mathbf{P}\mathbf{w} \le 0$$

So, the adaptation rule is as follows:

$$\frac{\mathrm{d}m_F(t)}{\mathrm{d}t} = \frac{\gamma}{b}\mathbf{e}^{\mathrm{T}}\mathbf{P}b_ce \tag{24}$$

Lemma 4: The generalised adaption rule of the HF domain FOPID controller for the system defined in (5) is given in (24). The adaptation rule of the each individual component of the adaptive HF domain FOPID controller can be found using Lemma 1.

Proof: Now, with the help of (22) and (24), the SHF domain representation of adaptation rule is

$$\mathrm{diag}\left(\mathbf{M}_S\mathbf{D}_{\mathrm{FS}}^{\mathrm{l}}\right) = \mathrm{diag}(\frac{\gamma}{b}\mathbf{E}_S^T\mathbf{P}b_c\mathbf{E}_{1S}) \tag{25}$$

and in the TF domain part of the adaptive FOPID controller is

$$\begin{aligned}&\mathrm{diag}(\mathbf{M}_S\mathbf{D}_{\mathrm{FS}}^{\mathrm{l}} + 2\mathbf{M}_T\mathbf{D}_{\mathrm{FT}}^{\mathrm{l}})\\ &\quad= \frac{\gamma}{b}\mathrm{diag}(\mathbf{E}_S^T\mathbf{P}b_c\mathbf{E}_{1T} + \mathbf{E}_T^T\mathbf{P}b_c\mathbf{E}_{1S} + \mathbf{E}_T^T\mathbf{P}b_c\mathbf{E}_{1T})\end{aligned} \tag{26}$$

These two adaptation rules show that the value of operational matrix of FOPID can be evaluated in terms of adaptation parameter γ, error state vector $\mathbf{e}(t)$, Lyapunov martrix $\mathbf{P}$, output coefficient matrix b_c and tracking error $e(t)$. So, it is evident that the

Table 1 Sample insertion technique for FOPID controller in HF domain

Sampling instant	Distribution of samples	Time period
1	$[0 \ \ 0 \ \ 0 \ \ \cdots \ \ 0 \ \ f_0]$	h_F^q
2	$[0 \ \ 0 \ \ 0 \ \ \cdots \ \ f_0 \ \ f_1]$	h_F^q
$\vdots$	$\vdots$	$\vdots$
$m-2$	$[0 \ \ 0 \ \ f_0 \ \ \cdots \ \ f_{m-4} \ \ f_{m-3}]$	h_F^q
$m-1$	$[0 \ \ f_0 \ \ f_1 \ \ \cdots \ \ f_{(m-3)} \ \ f_{(m-2)}]$	h_F^q
m	$[f_0 \ \ f_1 \ \ f_2 \ \ \cdots \ \ f_{(m-2)} \ \ f_{(m-1)}]$	h_F^q
$m+1$	$[f_1 \ \ f_2 \ \ f_3 \ \ \cdots \ \ f_{(m-1)} \ \ f_m]$	h_F^q
$m+2$	$[f_2 \ \ f_3 \ \ f_4 \ \ \cdots \ \ f_m \ \ f_{(m+1)}]$	h_F^q
$m+3$	$[f_3 \ \ f_4 \ \ f_5 \ \ \cdots \ \ f_{(m+1)} \ \ f_{(m+2)}]$	h_F^q
$\vdots$	$\vdots$	$\vdots$

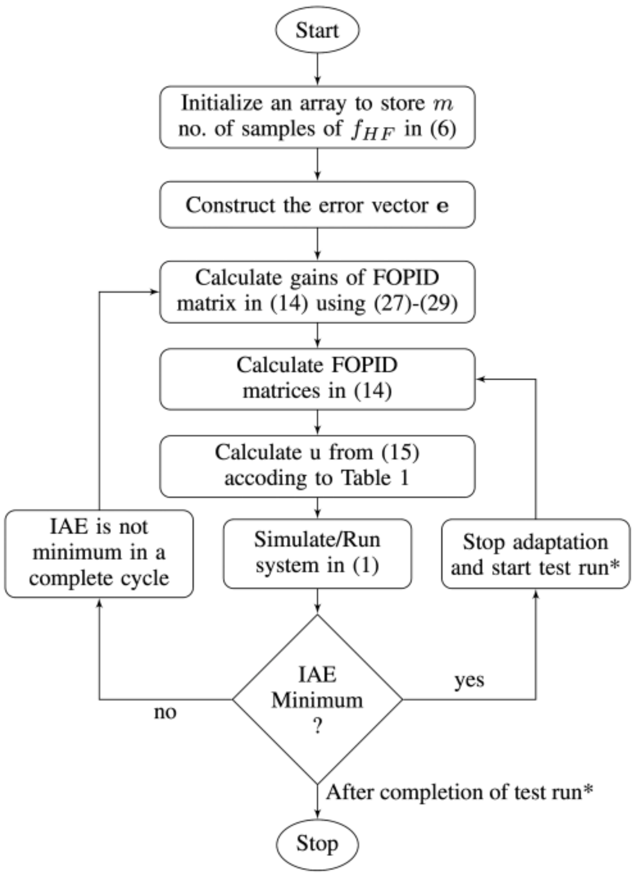

Fig. 2 *Flowchart representation of the adaptive FOPID controller in the HF domain*

calculation of the gamma function is not required to evaluate the adaptive FOPID matrix.

- *Adaptation rule for proportional controller:* The adaptation rule for the proportional controller can be derived from the adaptation rule of the FOPID controller in (25) is as follows:

$$\left[\frac{\mathrm{d}}{\mathrm{d}t} m_{\mathrm{FP}}(t)\right] \triangleq \left(\mathbf{M}_{\mathrm{SFP}} \mathbf{D}_{\mathrm{FS}}^{1}\right)_{ii} = \gamma_P \mathbf{E}_{S_{ii}}^{\mathrm{T}} \mathbf{P}_{ii} b \mathbf{E}_{1S_i} \tag{27}$$

  where $i = 1, 2, 3\ldots, m+1$ and γ_P is the learning factor of the proportional controller.
- *Adaptation rule for integral controller:* The adaptation rule for the integral controller can derived from the adaptation rule of the FOPID controller in (25) is as follows:

$$\left[\frac{\mathrm{d}}{\mathrm{d}t} m_{\mathrm{FI}}(t)\right] \triangleq \left(\mathbf{M}_{\mathrm{SFI}} \mathbf{D}_{\mathrm{FS}}^{1}\right)_{ii} = \gamma_I \mathbf{E}_{S_{ii}}^{\mathrm{T}} \mathbf{P}_{ii} b \mathbf{E}_{1S_i} \tag{28}$$

  where $i = 1, 2, 3\ldots, m+1$ and γ_I is the learning factor of the integral controller.
- *Adaptation rule for derivative controller:* The adaptation rule for the derivative controller can derived from the adaptation rule of the FOPID controller in (25) is as follows:

$$\left[\frac{\mathrm{d}}{\mathrm{d}t} m_{\mathrm{FD}}\right] \triangleq \left(\mathbf{M}_{\mathrm{SFD}} \mathbf{D}_{\mathrm{FS}}^{1}\right)_{ii} = \gamma_D \mathbf{E}_{S_{ii}}^{\mathrm{T}} \mathbf{P}_{ii} b \mathbf{E}_{1S_i} \tag{29}$$

  where $i = 1, 2, 3\ldots, m+1$ and γ_D is the learning factor of the derivative controller.

□

4.2 Implementation technique of the FOPID controller in the NSOF domain

In this section, new implementation techniques of non-causal convolution in terms of samples is introduced in the NSOF domain. The adaptation rules of FOPID controller require only samples of the state vector. So, the FOPID matrix in the NSOF domain can be represented in terms of samples only. Now, for the evaluation of control signal, the sample selection technique is discussed here. A window of m number of samples are selected with h_F^q sampling time-period which must consider a minimum approximation error.

As shown in Table 1, the continuous counter-clockwise rotation of samples, insert the new samples in the windows. So, this dynamic behaviour of the sample window always takes care of new samples as well as serves the purpose of non-causal convolution. The approximated control signal for system in (5) is calculated based on Lemmas 1 and 4 as shown in the flowchart in Fig. 2. In this technique, the present sample always gets the highest priority to contribute more for improving the system performance and past signals are getting less importance on the basis of the fractional order of the integration or differential as discussed in Sections 3 and 4.

5 Result and discussion

5.1 Simulation case studies

5.1.1 Case study 1.: The unforced second-order Duffing's oscillatory system is chaotic in nature but this special class of non-linear system is linearisable with the help of feedback linearisation technique [4]. The dynamic model of the Duffing's oscillatory system is defined as

$$\begin{cases} \dot{x}_1(t) = x_2(t) \\ \dot{x}_2(t) = -x_1^3(t) - 0.1x_2(t) + 12\cos(t) + u(t) + d(t) \\ y(t) = x_1(t) \end{cases} \tag{30}$$

Now, with help of different variants of the HF domain FOPID controller as discussed Section 4, the feedback linearisation technique is applied on Duffing's oscillatory system for tracking a pure sinusoidal reference signal of amplitude 1 unit with periodicity of 5 s (i) without any disturbance, i.e. $d(t) = 0$ (ii) with an external disturbance such as square wave with random height within the range $[-1, 1]$ and a period of 0.5 s.

Comparison of design strategies: Here, our prime objective is to train the HF domain adaptive FOPID controller for Duffing's oscillatory system. The system is simulated using RK4 method for 10 s with a sampling time period of 0.01 s. The tuning technique of the proposed controller, which is discussed in Section 4.2 is implemented here. Also, the performance of the conventional or the HF domain FOPID/PID controllers is measured for the same objective. Then the results of the simulation study for both of the reference signals with the different variants of the FOPID controller are discussed here to evaluate the effectiveness of the proposed controller.

Table 2 Comparision of IAE for different variants of the FOPID controller in case study 1

Duffing's system	Controller	PID	FOPID
	conventional	2.7841	3.9832
without	HF domain	2.0172	0.4955
disturbance	adaptive HF domain	0.1691	0.0200
	conventional	1.9336	2.0375
with	HF domain	2.9343	0.2497
disturbance	adaptive HF domain	0.0793	0.0242

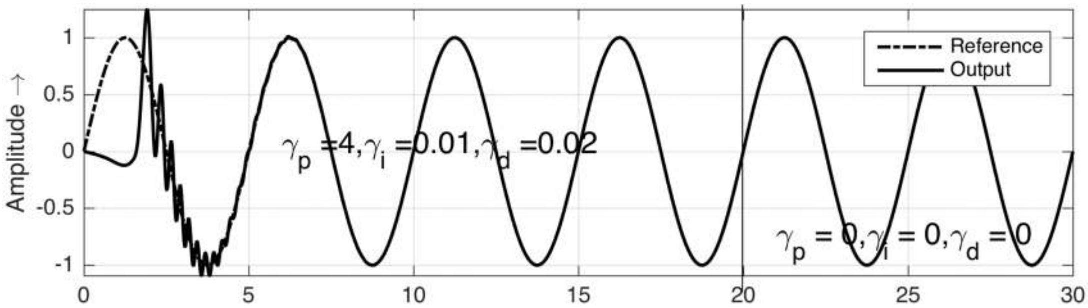

Fig. 3 *Performance characteristics of the Duffing's system without disturbance with the HFAFOPID controller*

- *PID and FOPID:* The FOPID/PID controller is implemented via convolution integral using the GL method including short-term memory concept. These controllers are tuned via particle swarm optimisation (PSO) using the following method. The desired transient and steady-state specification are achieved by providing the approximated range of $K_\mathrm{P}, K_\mathrm{I}, K_\mathrm{D}, \alpha$ and β to PSO to reduce the tracking error for which the IAE is minimum. The values of $(\alpha, \beta) \equiv$ (i) $(-0.4767, 0.4336)$ (ii) $(-0.8184, 0.6750)$ are calculated from this study for Duffing's oscillatory system (i) without disturbance and (ii) with external disturbance, respectively. It shows that the more memory power of integrator and differentiator is required to reject the external disturbance. These values of (α, β) are used for rest of the variants of the FOPID controllers. Now, after the simulation, the values of the IAE which are listed in Table 2 for both of the cases indicate the limitations of the conventional FOPID/PID controller.
- *HFPID and HFFOPID:* The structure of the HF domain FOPID/PID controllers are defined in Lemma 2. It is easy to implement and memory consumption during simulation is easily controllable by the proper selection of the HF domain component function. The stable NSOF domain FOPID/PID controllers are tuned for both of the reference signals separately via PSO with 20 particles and 10 iterations. Only the parameters $K_\mathrm{P}, K_\mathrm{I}, K_\mathrm{D}$ are tuned and values of α, β are selected from the previous case. As stated earlier, the effectiveness of the HF domain FOPID/PID controller also depends on the selection of the components function of the HF domain. Along with the five parameters of the NSOF domain controller, the number of component functions in the HF domain can also be considered as the variable during the simulation study. The proper choice of the HF components depends on (i) minimum approximation error and (ii) less time and memory consumption during simulation which is already discussed in Section 2. The values of IAE in Table 2 also supports modification of implementation technique of the FOPID/PID controllers via the HF domain. Although the HF domain FOPID/PID controller is superior over the conventional FOPID/PID controller due to the lack of knowledge about the initial value of the parameters of the controller leads the system to the verge of instability.
- *HFAPID and HFAFOPID:* Applying Lyapunov redesign technique adaptation rules are synthesised for the HF domain-based adaptive FOPID/PID controllers. Here the controllers were trained for 20 s as shown in Fig. 3 or Fig. 4. The adapted parameters are used for a test run if the following conditions are satisfied individually or both together as (1) control signal satisfies the boundary conditions, (2) the IAE will saturate after a certain time. The parameters of HFAPID controller are chosen as

$$\mathbf{P} = \begin{bmatrix} 5 & 1 \\ 1 & 5 \end{bmatrix}.$$

The number of HF components is equal to 10 to provide minimum approximation errors. The adaptation values γ_p, γ_I and γ_D are set to provide good transient performance and then controller adapts the parameters to cancel steady-state error. The initial value of $K_\mathrm{P}, K_\mathrm{I}, K_\mathrm{D}$ is selected as zero and adopted values of the parameters are calculated from the simple integer-order adaptation rules given in (27)–(29) during the training period and IAE is calculated in each cycle. The adaptation is stopped when the value of IAE is saturated and the system performed the test run. Fig. 5*a* shows the nature of control signal during adaptation as well as test run period and the nature of error signal is shown in Fig. 5*b* for the plant in (30) without any disturbance. The nature of the control signal and error signal for the same plant with disturbance is shown in Figs. 6*a* and *b*, respectively. The results of simulation studies are tabulated in Table 2. In all these simulations, the plant is evaluated for 10 s after the training is completed by different adaptation strategies so as to compare the results. Among the competing controllers, the HFAPID scheme shows the best performance for both of the reference signals as it is evident from the IAE values in Table 2.

5.1.2 Case study 2.: A second-order linear DC motor with non-linear friction [4] is simulated here. The mathematical model is

$$\begin{cases} \dot{x}_1(t) = x_2(t) \\ \dot{x}_2(t) = -\dfrac{f(x_2(t))}{J} + \dfrac{C_T}{J}u(t) \\ y(t) = x_1(t) \end{cases} \tag{31}$$

$x_1(t)$ is the angular position of the rotor (in radians), x_2 is the angular speed (in radians per second), and u is the current fed to the motor (in amperes). The plant parameters are $C_T = 10\,\mathrm{NmA^{-1}}, J = 0.1\,\mathrm{kg\,m^2}$, and the non-linear friction torque is defined as $f(x_2) = 5\tan^{-1}(5x_2)\mathrm{Nm}$.

The control objective is to make the angular position y to follow a reference signal given by $\ddot{y}_m = 400w(t) - 40\dot{y}_m - 400y_m$ where $w(t)$ is a square wave of random amplitude that changes in the interval $(-1.5, 1.5)$ in every 0.5 s

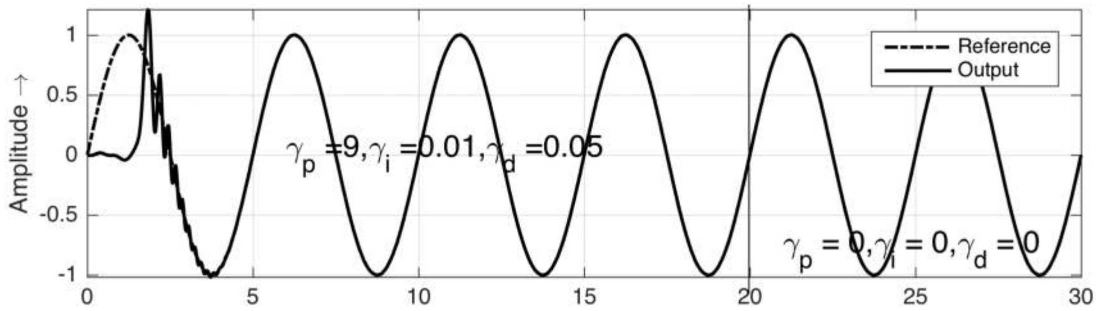

Fig. 4 *Performance characteristics of the Duffing's system with disturbance using the HFAFOPID controller*

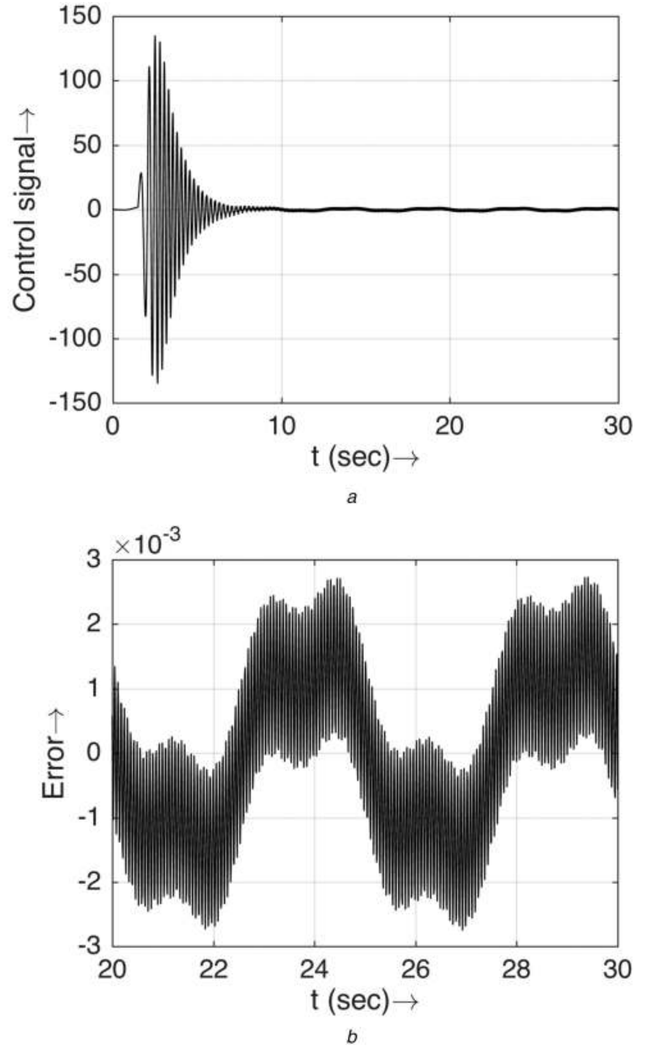

Fig. 5 *The control signal and error signal for Fig. 3, the Duffing's system without disturbance using HFAFOPID controller*
(a) control signal, ***(b)*** tracking error signal

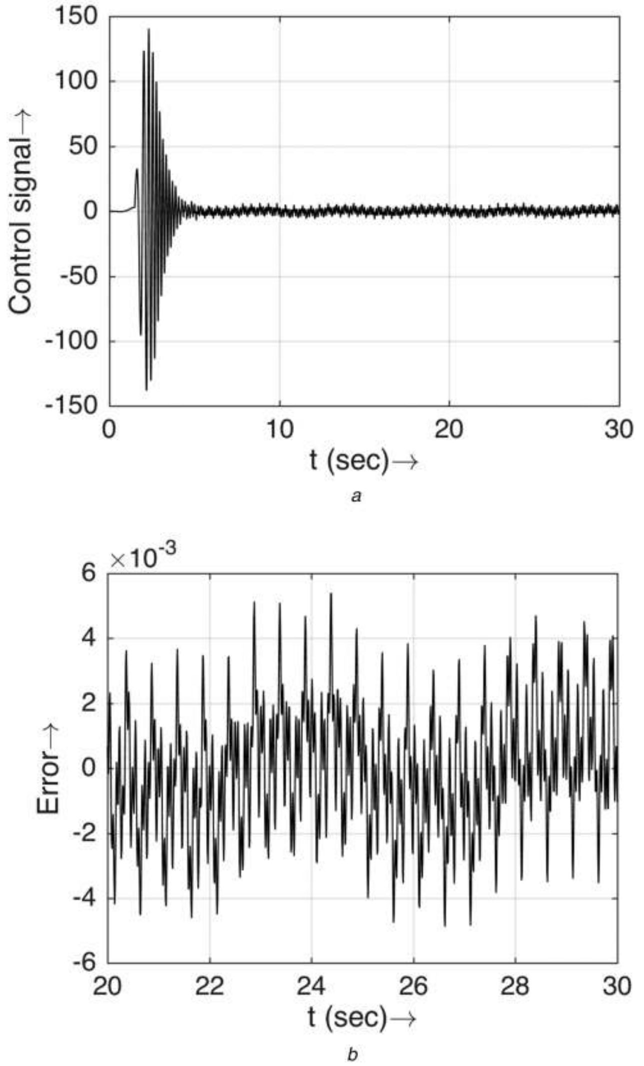

Fig. 6 *The control signal and error signal for Fig. 4, the Duffing's system with disturbance using HFAFOPID controller*
(a) control signal, ***(b)*** tracking error signal

Comparison of design strategies: The conventional, HF domain-based and HF domain-based adaptive FOPID/PID controller design strategies are implemented in a similar fashion as in the earlier case study.

Non-linear DC motor is simulated with the sampling time period of 0.01 s. The performance characteristics are shown in Fig. 7. In a similar fashion of case study 1, the values of $(\alpha, \beta) \equiv (-0.0086, 0.5829)$ are selected from conventional FOPID and is used for rest variants. In this case study also, as shown in Table 3, the HFAFOPID/HFAPOD design strategy emerges as the best solution. Hence, this design strategy evolves as the most superior solution from both the points of view of best performance and simplest implementation.

5.2 Experimental case study

5.2.1 Case study 3.: To demonstrate the effectiveness of the proposed controller, a real-life experiment [4] is considered where we attempt to perform the speed controlled of an armature controlled DC motor. The nameplate data of the motor is given in Table 4.

$$\begin{cases} \dot{x}_1(t) = x_2(t) \\ \dot{x}_2(t) = \left(\dfrac{fR_a}{JL_a} + \dfrac{k_b k_t}{JL_a}\right) + \left(\dfrac{f}{J} + \dfrac{R_a}{L_a}\right) + \dfrac{k_t}{JL_a}u(t) \\ y(t) = x_1(t) \end{cases} \tag{32}$$

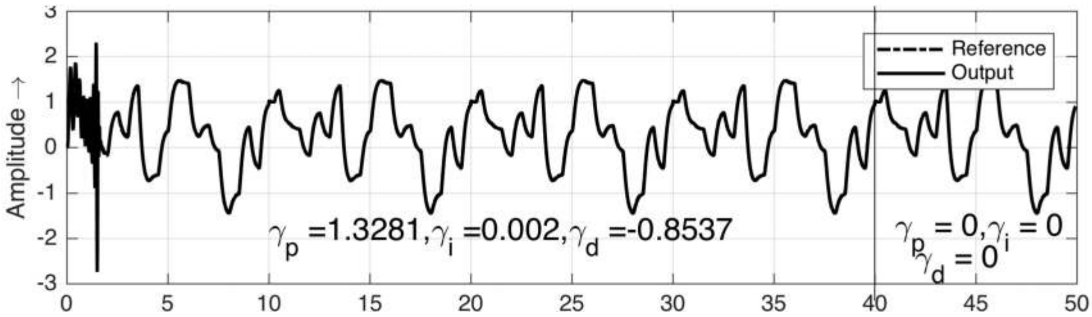

Fig. 7 *Performance characteristics of the non-linear DC motor of case study 2 using the HFAFOPID controller*

Table 3 IAE value of case study 2

Controller	PID	FOPID
conventional	0.2215	0.1905
HF domain	0.4626	0.5771
adaptive HF domain	0.1529	0.0537

Table 4 Nameplate data of DC motor setup in case study 4

armature voltage	50 V	type	DC
armature current	1.1 A	insulation	B
field excitation	50 V	frame	HB3

Table 5 IAE value of case study 3

Controller	PID	FOPID
conventional	3.1693×10^3	1.7270×10^3
HF domain	1.8699×10^3	2.1466×10^3
adaptive HF domain	1.6602×10^3	1.0440×10^3

The experimental setup is interfaced with a PC via Arduino Uno and controller are implemented digitally as shown in Fig. 8*a*. The second-order model of a DC motor in (32) is obtained using open loop data. The output y is the angular speed of the motor. Using simulation, parameters of different variants FOPID/PID are calculated in a similar manner of the previous case studies.

The values $\alpha = -0.7384$, $\beta = 0.3315$ are selected from the conventional FOPID controller.

In each of these experimentations, the speed measurement is carried out using tacho-generator which is mounted on the shaft with a resolution of 0.002 V/rpm. Then, the acquired speed signal is filtered in the software environment, employing a double pole filter (double pole at -20) to remove noise pickup. It can be seen that the controllers developed give satisfactory performance for a test run for 75 s and speed levels are 1000, 1500 and 1200 rpm with a load variation up to 50% with a pulse-width modulation duty cycle of 10 ms. Table 5, reveals that, in this real-life experiment also, HFAFOPID emerges as the best controller among the other variants.

5.2.2 Case study 4.: A non-linear plant, the robotic arm with two degrees of freedom, is introduced as an experimental setup. In order to show the effectiveness of the proposed controller, the tip of the end-effector is instructed to tracking a sinusoidal signal [26, 50]. Two servo motors at link 1 and link 2 are used here to control the absolute joint-angle. Here, θ_1 is the absolute joint angle at link 1 and θ_2 is the relative joint angle between link 1 and link 2. Now, $\theta_{12}(=\theta_1+\theta_2)$ is the absolute joint angle of link 2. The position of the end-effector is measured in (r, θ_r) co-ordinate system. Motor 1 and motor 2 provide torque to actuate two links simultaneously. These high torque standard servo motor with metal gears provides 35 kg/cm at 5 V. The motor angles or the absolute angles θ_1 and θ_{12} of the links are measured by the inbuilt rotary encoder of the servo motor.

The parameters of the links are as follows: $l_1 = 0.06\,\text{m}$, $m_1 = 0.15\,\text{kg}$ and $l_2 = 0.1\,\text{m}$, $m_2 = 0.03\,\text{kg}$. To implement controllers into the robotic manipulator, an Arduino mega is used as a data acquisition board with the sampling frequency of 10 kHz. The controller is realised in mac os-based operating system with 1.4 GHz Intel Core i5 processor and 4 GB DDR3 RAM. The dynamics of the motion of the two-link manipulator is given below:

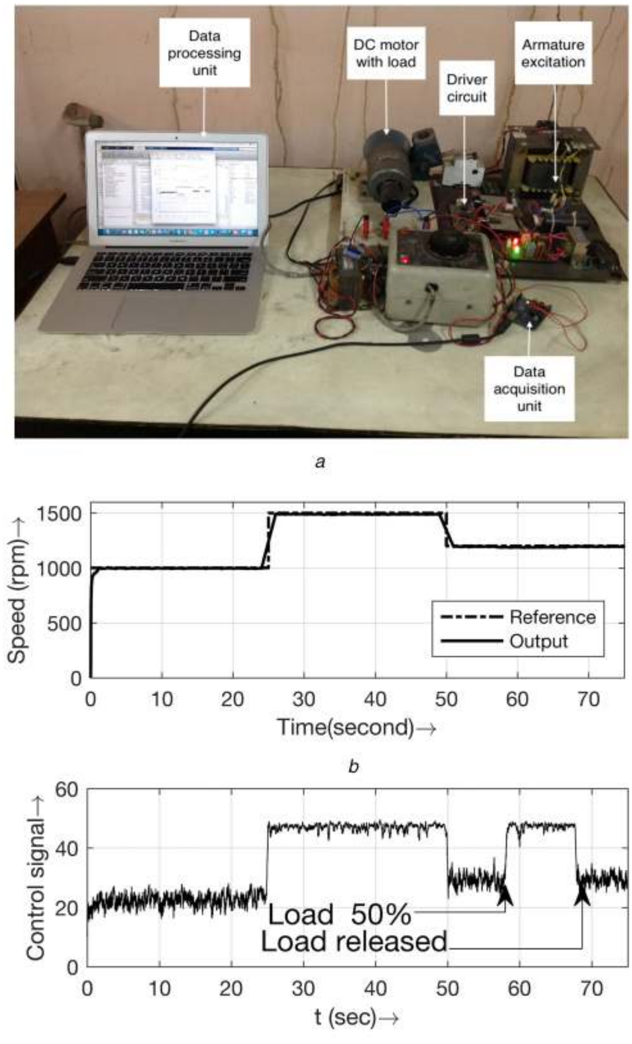

Fig. 8 *Implementation of HFAFOPID controller for real-life DC motor speed control system*

(a) Real-life PC-based experimental arrangement for the speed control of DC motor, ***(b)*** Performance characteristics of the real-life armature controlled DC motor when tracking variable speed with the HFAFOPID controller, ***(c)*** Control signal of the system defined in (32) with the HFAFOPID controller during test run period. This control signal shows the precise variation due to the change in the reference signal. The load variation is rejected by the controller smoothly which evident from Figs. 8*b* and *c*

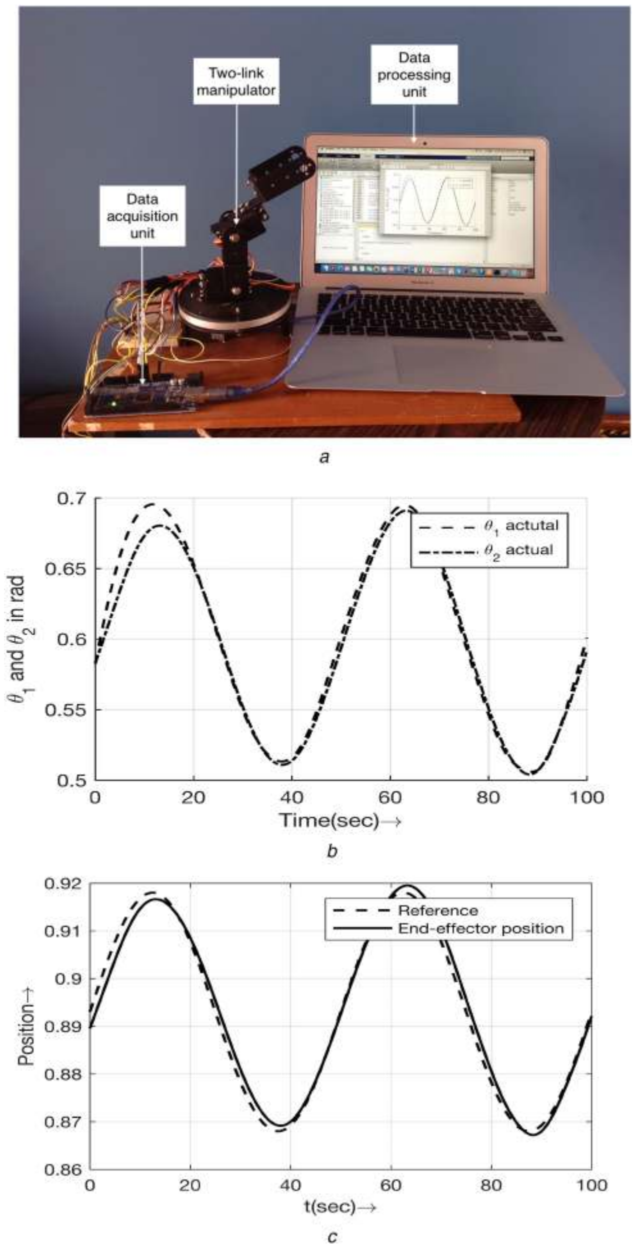

Fig. 9 ***(a)*** *Real-life PC-based experimental arrangement for the two-link manipulator,* ***(b)*** *Performance characteristics of the joint-angles of two-link manipulator defined (33) with the HFAFOPID controller when the frequency of the reference signal is 0.02 Hz,* ***(c)*** *Performance characteristics of the position of the end-effector of two-link manipulator defined (33) with the HFAFOPID controller when the frequency of the reference signal is 0.02 Hz*

$$\begin{cases} B(q)\ddot{q} + C(\dot{q}, q) + g(q) = F_\theta \\ q = [\theta_1, \theta_2]^{\mathrm{T}} \end{cases} \tag{33}$$

where

$$B(q) = \begin{bmatrix} (m_1 + m_2)l_1^2 + m_2 l_2^2 + 2m_2 l_1 l_2 \cos\theta_2 & m_2 l_2^2 + m_2 l_1 l_2 \cos\theta_2 \\ m_2 l_2^2 + m_2 l_1 l_2 \cos\theta_2 & m_2 l_2^2 \end{bmatrix}$$

$$C(\dot{q}, q) = \begin{bmatrix} -m_2 l_1 l_2 \sin\theta_2 (2\dot{\theta}_1 \dot{\theta}_2 + \dot{\theta}_2^2) \\ m_2 l_1 l_2 \sin\theta_2 \dot{\theta}_1 \dot{\theta}_2 \end{bmatrix}$$

$$g(q) = \begin{bmatrix} -(m_1 + m_2) g l_1 \sin\theta_1 - m_2 g l_2 \sin(\theta_1 - \theta_2) \\ m_2 g l_2 \sin(\theta_1 - \theta_2) \end{bmatrix}$$

$$r = \sqrt{l_1^2 + l_2^2 + 2l_1 l_2 \cos\theta_2}$$

Table 6 IAE value of case study 4

Reference	Controller	PID	FOPID
	conventional	0.4378	0.3058
0.02 Hz	HF domain	0.4087	0.3546
	adaptive HF domain	0.2564	0.2058
	conventional	4.1132	3.9734
0.1 Hz	HF domain	4.4007	3.3326
	adaptive HF domain	2.4058	2.2368

$$\theta_r = \tan^{-1}\left(\frac{l_1 \cos\theta_1 + l_2 \cos(\theta_1 + \theta_2)}{l_1 \sin\theta_1 + l_2 \sin(\theta_1 + \theta_2)}\right)$$

A pure sinusoidal signal with two different frequencies is applied separately as the reference position (r, θ_r) to verify the tracking performance of the proposed HF domain adaptive FOPID controller. In order to avoid the hardware constraints (range of θ_1 is 30°– 160° and θ_2 is 20°– 170°) and singular position, the reference signal is generated and control signal is restricted. Two FOPID controllers are used for two different joint angles which are given in Fig. 9*b*. All the variants of the FOPID controllers are tuned in software environment to control the position error based on the position feedback. The performance characteristics of the manipulator with the HFAFOPID controller is shown in Fig. 9*c*. The control performance is evaluated using the sinusoidal signals with two different frequencies, i.e. 0.02, 0.1 Hz. The corresponding IAE values with different variants of FOPID controllers are listed in Table 6. In this case study also, the HFAFOPID/HFAPOD design strategy emerges as the best solution from both the points of view of best performance and simplest implementation.

6 Conclusion

This paper has introduced a new approach for designing the FOPID controllers employing NSOFs. In this approach, a hybrid NSOF sets are utilised to describe the dynamics of the system when a fractional-order PID controller is connected in feedforward configuration with the plant. The alternative algebraic vector–matrix form of fractional-order dynamics in the NSOF domain employs to (i) find asymptotic stability condition of the overall system in the sense of Lyapunov, (ii) adapt the rules of the parameters of FOPID controller which are independent of gamma function and (iii) implement the techniques of the NSOF domain in the real-life problem. Also, the proposed adaptive FOPID design methodology does not require a prior knowledge about the plant to be controlled due to the adaptive nature of design and the fractional-order of error dynamics forms a continuous manoeuvreing of control law. The proposed hybrid NSOF-based non-adaptive and adaptive FOPID controller design strategies along with conventional PID and FOPID controllers are applied in simulation and real-life experimentation for the benchmark case studies. The adaptive hybrid model of FOPID design strategy is evolved as a superior technique as compared to the other strategies discussed in this paper.

7 References

[1] Atassi, A.N., Khalil, H.K.: 'A separation principle for the control of a class of nonlinear systems', *IEEE Trans. Autom. Control*, 2001, **46**, (5), pp. 742–746

[2] Isidori, A.: '*Nonlinear control systems*' (Springer Science & Business Media, London, 2013)

[3] Khalil, H.K.: 'Adaptive output feedback control of nonlinear systems represented by input-output models', *IEEE Trans. Autom. Control*, 1996, **41**, (2), pp. 177–188

[4] Sharma, K.D., Chatterjee, A., Rakshit, A.: 'A hybrid approach for design of stable adaptive fuzzy controllers employing Lyapunov theory and particle swarm optimization', *IEEE Trans. Fuzzy Syst.*, 2009, **17**, (2), pp. 329–342

[5] Han, J.: 'From PID to active disturbance rejection control', *IEEE Trans. Ind. Electron.*, 2009, **56**, (3), pp. 900–906

[6] Monje, C.A., Vinagre, B.M., Feliu, V., *et al.*: 'Tuning and auto-tuning of fractional order controllers for industry applications', *Control Eng. Pract.*, 2008, **16**, (7), pp. 798–812

[7] Åström, K.J., Hägglund, T.: 'PID controllers: theory, design, and tuning', 1995

[8] Åström, K.J., Hang, C.C., Persson, P., *et al.*: 'Towards intelligent PID control', *Automatica*, 1992, **28**, (1), pp. 1–9

[9] Erenturk, K.: 'Fractional-order PID controller and active disturbance rejection control of nonlinear two-mass drive system', *IEEE Trans. Ind. Electron.*, 2013, **60**, (9), pp. 3806–3813

[10] Ang, K.H., Chong, G., Li, Y.: 'Pid control system analysis, design, and technology', *IEEE Trans. Control Syst. Technol.*, 2005, **13**, (4), pp. 559–576

[11] Yamamoto, T., Takao, K., Yamada, T.: 'Design of a data-driven PID controller', *IEEE Trans. Control Syst. Technol.*, 2009, **17**, (1), pp. 29–39

[12] Yeroglu, C., Tan, N.: 'Note on fractional-order proportional–integral–differential controller design', *IET Control Theory Appl.*, 2011, **5**, (17), pp. 1978–1989

[13] Li, M., Li, D., Wang, J., *et al.*: 'Active disturbance rejection control for fractional-order system', *ISA Trans.*, 2013, **52**, (3), pp. 365–374

[14] Raynaud, H.F., Zergaınoh, A.: 'State-space representation for fractional order controllers', *Automatica*, 2000, **36**, (7), pp. 1017–1021

[15] Oustaloup, A., Cois, O., Lanusse, P., *et al.*: 'The crone aproach: theoretical developments and major applications', *IFAC Proc. Vol.*, 2006, **39**, (11), pp. 324–354

[16] Vinagre, B.M., Feliu, V.: 'Optimal fractional controllers for rational order systems: a special case of the wiener-hopf spectral factorization method', *IEEE Trans. Autom. Control*, 2007, **52**, (12), pp. 2385–2389

[17] Bode, H.W.: 'Relations between attenuation and phase in feedback amplifier design', *Bell Labs Tech. J.*, 1940, **19**, (3), pp. 421–454

[18] Oustaloup, A.: '*Crone control: robust control of non-integer order*' (Hermes, Paris, 1991)

[19] Podlubny, I.: 'Fractional-order systems and fractional order controllers', *IEEE Transactions on automatic control*, 1999, **44**, (1), pp. 208–214

[20] Merrikh Bayat, F., Karimi Ghartemani, M.: 'Method for designing fractional PID stabilisers for minimum-phase fractional-order systems', *IET Control Theory Appl.*, 2010, **4**, (1), pp. 61–70

[21] Valério, D., Da Costa, J.S.: 'Time-domain implementation of fractional order controllers', *IEE Proc., Control Theory Appl.*, 2005, **152**, (5), pp. 539–552

[22] Angel, L., Viola, J.: 'Design and statistical robustness analysis of FOPID, IOPID and SIMC PID controllers applied to a motor-generator system', *IEEE Latin Am. Trans.*, 2015, **13**, (12), pp. 3724–3734

[23] Pan, I., Das, S.: '*Intelligent fractional order systems and control: an introduction*' vol. **438**, (Springer, Berlin Heidelberg, 2012)

[24] Zhong, J., Li, L.: 'Tuning fractional-order PID controllers for a solid-core magnetic bearing system', *IEEE Trans. Control Syst. Technol.*, 2015, **23**, (4), pp. 1648–1656

[25] Folea, S., Muresan, C.I., De Keyser, R., *et al.*: 'Theoretical analysis and experimental validation of a simplified fractional order controller for a magnetic levitation system', *IEEE Trans. Control Syst. Technol.*, 2016, **24**, (2), pp. 756–763

[26] Dumlu, A., Erenturk, K.: 'Trajectory tracking control for a 3-dof parallel manipulator using fractional-order PID control', *IEEE Trans. Ind. Electron.*, 2014, **61**, (7), pp. 3417–3426

[27] Moshrefi Torbati, M., Hammond, J.: 'Physical and geometrical interpretation of fractional operators', *J. Franklin Inst.*, 1998, **335**, (6), pp. 1077–1086

[28] Podlubny, I.: 'Geometric and physical interpretation of fractional integration and fractional differentiation', *Fract. Calc. Appl. Anal.*, 2002, **5**, (4), pp. 367–386

[29] Podlubny, I.: 'Matrix approach to discrete fractional calculus', *Fract. Calc. Appl. Anal.*, 2000, **3**, (4), pp. 359–386

[30] Chang, P.H., Jung, J.H.: 'A systematic method for gain selection of robust pid control for nonlinear plants of second-order controller canonical form', *IEEE Trans. Control Syst. Technol.*, 2009, **17**, (2), pp. 473–483

[31] Sastry, S.S., Isidori, A.: 'Adaptive control of linearizable systems', *IEEE Trans. Autom. Control*, 1989, **34**, (11), pp. 1123–1131

[32] Landau, I.D., Lozano, R., M'Saad, M., *et al.*: '*Adaptive control: algorithms, analysis and applications*' (Springer Science & Business Media, London, 2011)

[33] Wiese, D.P., Annaswamy, A.M., Muse, J.A., *et al.*: 'Adaptive output feedback based on closed-loop reference models for hypersonic vehicles', *J. Guid. Control Dyn.*, 2015, **38**, (12), pp. 2429–2440

[34] Gibson, T.E., Annaswamy, A.M., Lavretsky, E.: 'On adaptive control with closed-loop reference models: transients, oscillations, and peaking', *IEEE Access*, 2013, **1**, pp. 703–717

[35] Benaskeur, A.R., Desbiens, A.: 'Backstepping-based adaptive PID control', *IEE Proc., Control Theory Appl.*, 2002, **149**, (1), pp. 54–59

[36] Huang, H.P., Roan, M.L., Jeng, J.C.: 'On-line adaptive tuning for PID controllers', *IEE Proc., Control Theory Appl.*, 2002, **149**, (1), pp. 60–67

[37] Li, Y., Chen, Y., Podlubny, I.: 'Stability of fractional-order nonlinear dynamic systems: Lyapunov direct method and generalized mittag–leffler stability', *Comput. Math. Appl.*, 2010, **59**, (5), pp. 1810–1821

[38] Trigeassou, J.C., Maamri, N., Sabatier, J., *et al.*: 'A lyapunov approach to the stability of fractional differential equations', *Signal Process.*, 2011, **91**, (3), pp. 437–445

[39] Sannuti, P.: 'Analysis and synthesis of dynamic systems via block-pulse functions'. *Proc. Inst. Electr. Eng.*, 1977, **124**, (6), pp. 569–571

[40] Deb, A., Sarkar, G., Bhattacharjee, M., *et al.*: 'A new set of piecewise constant orthogonal functions for the analysis of linear siso systems with sample-and-hold', *J. Franklin Inst.*, 1998, **335**, (2), pp. 333–358

[41] Sarkar, G., Dasgupta, A., Deb, A.: 'Microprocessor-based simulation of sampled data systems with/without a hold device using a set of sample-and-hold functions and dirac delta functions', *J. Franklin Inst.*, 2005, **342**, (1), pp. 85–95

[42] Deb, A., Sarkar, G., Sengupta, A.: '*Triangular orthogonal functions for the analysis of continuous time systems*' (Anthem Press, London, New York, 2011)

[43] Deb, A., Sarkar, G., Mandal, P., *et al.*: 'Transfer function identification from impulse response via a new set of orthogonal hybrid functions (hf)', *Appl. Math. Comput.*, 2012, **218**, (9), pp. 4760–4787

[44] Deb, A., Roychoudhury, S., Sarkar, G.: 'System identification: parameter estimation of transfer function', *Analysis and identification of time-invariant systems, time-varying systems, and multi-delay systems using orthogonal hybrid functions*' (SpringerNature, Switzerland, 2016), pp. 331–355

[45] Deb, A., Sarkar, G., Ganguly, A., *et al.*: 'Approximation, integration and differentiation of time functions using a set of orthogonal hybrid functions (hf) and their application to solution of first order differential equations', *Appl. Math. Comput.*, 2012, **218**, (9), pp. 4731–4759

[46] Wang, L.X.: 'Stable adaptive fuzzy control of nonlinear systems', *IEEE Trans. Fuzzy Syst.*, 1993, **1**, (2), pp. 146–155

[47] Oldham, K., Spanier, J.: '*The fractional caleulus*' (Academic Press, New York, 1974)

[48] McBride, A., Sabatier, J., Agrawal, O., *et al.*: 'Advances in fractional calculus: theoretical developments and applications in physics and engineering', 2008

[49] Baleanu, D., Machado, J.A.T., Luo, A.C.: '*Fractional dynamics and control*' (Springer Science & Business Media, New York, 2011)

[50] Oh, S., Kong, K.: 'Two-degree-of-freedom control of a two-link manipulator in the rotating coordinate system', *IEEE Trans. Ind. Electron.*, 2015, **62**, (9), pp. 5598–5607